



Nonequilibrium electron spectroscopy of Luttinger liquids

S. Takei, M. Millettari, and B. Rosenow

Max-Planck-Institut für Festkörperforschung, D-70569 Stuttgart, Germany

(Received 2 July 2010; published 22 July 2010)

We theoretically study a Luttinger liquid (LL) driven out of equilibrium by injection of high-energy electrons. The electrons are injected into the LL locally at a fixed energy and their spectral properties are detected at another spatial point some distance away by evaluating the average tunneling current from the LL into a resonant level with tunable energy. For energies slightly below the injection energy, the dependence of the detected current on the difference between injection, and detection energies is described by a power law whose exponent depends continuously on the Luttinger parameter. In contrast, for tunneling into a chiral LL edge of a fractional quantum-Hall state from the Laughlin sequence, we find that the detected current grows linearly with energy difference, despite a decreasing density of states.

DOI: [10.1103/PhysRevB.82.041306](https://doi.org/10.1103/PhysRevB.82.041306)

PACS number(s): 73.43.Jn, 71.10.Pm, 73.21.Hb

Understanding the effects of nonequilibrium on strongly interacting quantum systems is a challenging problem in condensed matter physics. Electrons in one dimension are known to form a strongly correlated phase of matter called a Luttinger liquid (LL), whose low-energy excitations are collective density waves, or plasmons, of the electron gas. Over the last decade, experimental advances in nanostructure fabrication have brought a resurgence of interest in the LL model because of the possibility to test its peculiar predictions.^{1–5} Defining signatures of a LL such as spin-charge separation,^{6,7} charge fractionalization,^{8,9} and power-law suppression of the local electron tunneling density of states^{10–14} have been experimentally verified. Recently, many works have considered LLs driven far from equilibrium^{15–20} in order to shed light on possible energy relaxation processes that have not been apparent in the above-mentioned equilibrium experiments.

Energy relaxation in a homogeneous LL is not expected due to a fundamental feature of the model: its integrability. This precludes thermalization of the system from an arbitrary excited state. Here we consider injecting electrons far away from any contacts at a fixed energy. Their spectral properties are extracted at another spatial point some distance away by evaluating the average tunneling current from the LL into an empty resonant level with tunable energy, a technique used recently to measure the energy distribution function of a chiral Fermi liquid.²¹ In this work, we consider both standard (nonchiral) and chiral LLs, which are realized at the edge of fractional quantum-Hall systems.^{3,4,12–14}

The main thrust of this work is that high energy electrons injected locally into a homogeneous LL can indeed relax. The relaxation is possible because the locality of the injection process allows the injected electrons to emit plasmons in the vicinity of the tunneling sites through a series of virtual states. For the standard LL and for probe energies slightly below the injection energy, we find that the inelastic component of the current shows a power-law behavior as a function of the difference between injection and detection energies with an exponent that continuously evolves as the interaction parameter is varied. Here, relaxation is possible due to the locality of the injection and detection processes which break translational symmetry. We develop a perturbative approach

to show how injected electrons can relax by emitting plasmons inside the wire. For a chiral LL at the edge of a fractional quantum-Hall state from the Laughlin sequence, an essentially exact calculation shows that the inelastic part of the electron current *increases* in a linear fashion as the probe energy is lowered from the injection energy toward the chemical potential of the edge state, despite a *decreasing* tunneling density of states for electrons. This behavior is compatible with our result for the standard LL in the limit of strongly repulsive interactions. For probe energies close to the chemical potential, the chiral LL is far from equilibrium: the electron spectral function approaches a finite value, in striking contrast to the power law decrease toward zero in equilibrium. In addition to the inelastic contribution to the probe current, there always is an elastic contribution for a chiral LL, indicating that a finite fraction of electrons travels from the injection to the probe site without losing energy.

Electrons with charge e_0 are injected into a LL from a resonant level (source) with energy $E_1 \equiv e_0 V_1 > 0$ at position $x=0$ (see Fig. 1). Energy relaxation is studied by coupling a second resonant level (probe) with energy $E_2 \equiv e_0 V_2 > 0$ to the LL at position $x=L$ (downstream for the chiral LL) and by computing the tunneling electron current between the LL and that level. The two levels are coupled to the LL via tunneling amplitudes η_1 and η_2 , respectively. In addition, source and probe dots are coupled to reservoirs held at chemical potentials μ_1 and μ_2 via tunneling amplitudes λ_1

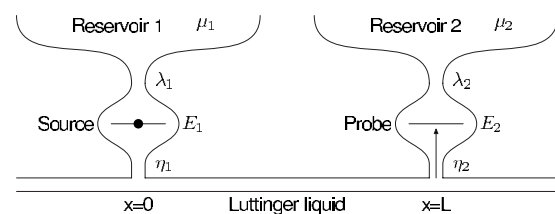


FIG. 1. A diagram of the setup considered. Hot electrons are injected from the source resonant level at $x=0$ and are collected at the probe resonant level at $x=L$. System parameters are set (see text) so that the source (probe) occupancy is fixed to be full (empty). Spectral properties of the injected electrons are extracted by measuring the tunneling current between the edge and the probe (indicated by the arrow).

and λ_2 . The chemical potential of the LL is taken to be zero. We assume the level broadening due to tunnel couplings to be small in comparison to both E_1 and E_2 , and therefore consider the current in the sequential-tunneling regime. Further, we assume $\lambda_1 \gg \eta_1$ with $\mu_1 > E_1$ so that the source occupancy is constrained to one and $\lambda_2 \gg \eta_2$ with $\mu_2 < E_2$ so that the probe occupancy is fixed at zero. We first focus on the standard LL and consider spinless electrons, for which the interaction strength is described by a single parameter K .² The case $K=1$ describes noninteracting electrons, $K < 1$ corresponds to repulsive interactions, and $K > 1$ to attractive ones. The system is modeled by the Hamiltonian $H=H_{LL}+H_{\text{dot}}+H_{\text{tun}}$, where H_{LL} models the LL, $H_{\text{dot}}=E_1\psi_1^\dagger\psi_1+E_2\psi_2^\dagger\psi_2$ the two resonant states, and H_{tun} describes the tunneling of electrons between the wire and the two resonant levels. ψ_1 (ψ_2) are electron operators of the source (probe) with occupation numbers $\langle\psi_1^\dagger\psi_1\rangle=1$ and $\langle\psi_2^\dagger\psi_2\rangle=0$. The standard LL Hamiltonian reads²

$$H_{LL}=\frac{u}{4\pi K}\int dx\{[\partial_x\phi_R(x)]^2+[\partial_x\phi_L(x)]^2\}, \quad (1)$$

where the left- and right-moving boson operators satisfy $[\phi_R(x),\phi_R(x')]=-\phi_L(x),\phi_L(x')]=i\pi K\text{sgn}(x-x')$. One-dimensional electron densities are given by $\rho_{R,L}(x)=\pm[\partial_x\phi_{R,L}(x)]/2\pi$ and u denotes the plasmon velocity. To simplify the notation, we use the units where $\hbar=1$ and $k_B=1$. The tunneling Hamiltonian is given by

$$H_{\text{tun}}=\eta_1\psi_1\psi^\dagger(x=0)+\eta_2\psi_2\psi^\dagger(x=L)+\text{H.c.}, \quad (2)$$

where $\psi(x)=\psi_R(x)+\psi_L(x)$. The electron operators can be bosonized as $\psi_{R,L}(x)=\exp\{i[K_\pm\phi_R(x)+K_\mp\phi_L(x)]\}/\sqrt{2\pi\alpha}$ with $K_\pm=(K^{-1}\pm 1)/2$ and α is the short distance cutoff of the theory. The expectation value of the current is given by $I=\langle T_c\{\hat{I}_{cl}(t_1)e^{-i\int_c dt H_{\text{tun}}(t)}\}\rangle_0$, where all operators are written in the interaction picture with respect to $H_{LL}+H_{\text{dot}}$. The current is computed using the nonequilibrium Keldysh technique²² and T_c indicates time ordering of the operators on the time-loop contour c . The ‘‘classical’’ component of the current operator is the symmetric combination of the operator on the forward (+) and backward (−) parts of the Keldysh contour, i.e., $\hat{I}_{cl}(t)=[\hat{I}_+(t)+\hat{I}_-(t)]/2$, where $\hat{I}_\pm(t)=-ie_0[H_\pm+\psi_{2,\pm}^\dagger\psi_{2,\pm}]$. If the propagation time L/u between the dots is much larger than the maximum of the dwell times $\tau_i=1/(\lambda_i^2+\eta_i^2)$, processes at the probe dot occur at later times than processes at the source dot, and the time ordering on the Keldysh contour is fixed accordingly.²³ To leading order in η_1 and η_2 , the steady state current is given by

$$I=e_0|\eta_1|^2|\eta_2|^2\int d^3te^{-iE_2t_2+iE_1t_34}[iG_{2\gamma+1}^<(-t_2)][iG_{2\gamma+1}^>(t_34)]\times\{\Pi_{1+\gamma}^<>-\Pi_{1+\gamma}^<<+\Pi_\gamma^<>-\Pi_\gamma^<<+2\Pi_{\gamma'}^<>-2\Pi_{\gamma'}^<<\}, \quad (3)$$

where $\gamma=K^2K$, $\gamma'=(K^2+K)K$, and $t_{ij}=t_i-t_j$. The factors of Green’s functions

$$iG_\beta^\pm(t)=\pm\frac{1}{2\pi\alpha}[\sin\pi T(\alpha/u\pm it)]^\beta \quad (4)$$

can be interpreted as the tunneling in and out density of states and the Π matrices

$$\Pi_\beta^{\rho\sigma}=\frac{G_\beta^\rho(t_{23})G_\beta^\sigma(-t_4)}{G_\beta^\rho(-t_3)G_\beta^\sigma(t_{24})} \quad (5)$$

describe the propagation of electrons along the wire. We neglect here the term proportional to $|\eta_2|^2$ since, for low temperatures ($T\ll E_1, E_2$), this contribution is exponentially suppressed.

When directly computing the tunneling current, the propagation matrices Π contain both left- and right-moving Green’s functions. In the limit where $L\gg u/\Delta E$, all dependence on left-moving Green’s functions cancels out. As a consequence, all propagators are right moving and only depend on the difference $L-ut$. Since all propagation times t are integrated over, the L dependence disappears by shifting the integration variables appropriately. The fact that the tunneling current is finite in the limit of $L\gg u\tau_i, u/\Delta E$ is due to the integrability of the LL model, which implies that the excitations propagate freely between the dots.

Denoting the energy loss by $\Delta E=E_1-E_2$, the leading contribution to the current for small $\Delta E\ll E_1$ at zero temperature reads

$$I=-\frac{2\pi e_0}{\hbar}\frac{|\eta_1|^2|\eta_2|^2\theta(\Delta E)}{u^2\hbar^2E_1\Gamma^2(1+\gamma)}\left(\frac{\alpha E_1}{u\hbar}\right)^{4\gamma}\left[\frac{(\Delta E/E_1)^{2\gamma-1}}{\Gamma(2\gamma)}\right]. \quad (6)$$

Here, $\Gamma(x)$ is the gamma function and we have reinstated \hbar for completeness. In the noninteracting limit ($\gamma\rightarrow 0$) the quantity in the square brackets is a representation of the delta function and Eq. (6) reduces to $I\propto\delta(\Delta E)$. When the interactions are turned on, the elastic peak gradually broadens to give rise to an inelastic contribution which shows a power law decay as a function of increasing ΔE with an exponent that continuously evolves as a function of the interaction parameter. For strong enough interactions with $\gamma > 1/2$, the elastic peak vanishes and the remaining inelastic contribution monotonically increases with a power law which again evolves as a function of the interaction parameter. The result Eq. (6) is plotted in Fig. 2. Broadening of the peak is included in the figure to reflect the finite width of the resonant levels due to the couplings to the reservoirs and the wire.

The physical origin behind the energy relaxation as described by Eq. (6) can be developed using lowest order perturbation theory in the limit of weak interactions with K close to 1. Interactions can be decomposed into forward scattering between electrons near the same Fermi point with amplitude g_4 and between electrons near opposite Fermi points with amplitude g_2 . The g_4 interaction merely renormalizes the fermion and plasmon velocities and cannot give rise to relaxation. In a spatially homogeneous LL, the g_2 process cannot give rise to energy relaxation either due to the simultaneous requirement of momentum and energy conservation. However, because of the local nature of injection and collection processes considered here, an electron is capable of ex-

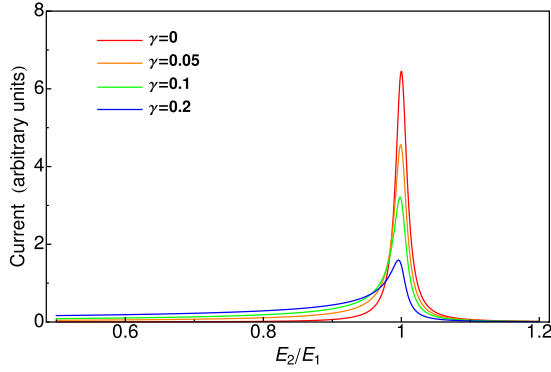


FIG. 2. (Color online) Tunneling current at the probe for the standard LL at zero temperature and for various interaction parameters. It includes the leading contribution in $\Delta E/E_1$. A level broadening of $0.01E_1$ is used for the elastic peak.

ploring virtual momentum states in connection with tunneling, and consecutive inelastic processes can both conserve momentum and produce a final state with the same total energy as the initial state.

To develop this picture in more detail, we begin by defining the noninteracting Hamiltonian (H_0) and the perturbation (H_{int}). The free Hamiltonian describes the right- and left-chiral fermions, $H_0 = u \int dx [\psi_R^\dagger(x) i \partial_x \psi_R(x) - \psi_L^\dagger(x) i \partial_x \psi_L(x)]$, where ψ_R, ψ_L denote right- and left-moving fermions, respectively. The interaction between the two species of fermions is described by $H_{g_2} = g_2 \int dx \psi_R^\dagger(x) \psi_R(x) \psi_L^\dagger(x) \psi_L(x)$. We assume that the effects of the g_4 interaction are encoded in the renormalized velocity u . The tunneling between the dots and the wire is still described by Eq. (2). The perturbation is then given by $H_{\text{int}} = H_{\text{tun}} + H_{g_2}$.

Here, we consider the lowest order inelastic process proportional to $\gamma \propto g_2^2$ at zero temperature, in which an electron is transported from the source to the probe while emitting a single plasmon inside the wire. Initially, the electron in the source ($|i\rangle = \psi_i^\dagger |0\rangle$) tunnels into a right-moving momentum eigenstate whose energy may be different from E_1 . In the second step, a left-moving plasmon with energy ΔE is emitted via a g_2 process and the right-moving electron is scattered into another wire state such that momentum is conserved. After propagating along the wire, the electron tunnels into the probe ($|f\rangle = \psi_f^\dagger b_p^\dagger |0\rangle$). Alternatively, tunneling into the wire can be elastic and the plasmon can be emitted when tunneling into the probe. The plasmon creation operator is defined as $b_p^\dagger = |p|^{-1/2} \int \frac{dk}{2\pi} \psi_L^\dagger(k+p) \psi_L(k)$, where $p < 0$ is the momentum of the emitted plasmon, and $E_{\text{pl}}(p) = u|p|$ is its energy. The square of the effective matrix element for this process can be evaluated by third-order perturbation theory

$$|\langle f|i\rangle_{\text{eff}}|^2 = g_2^2 |\eta_1 \eta_2^*|^2 \frac{\theta(-p)}{4\pi|p|(\hbar u)^4}, \quad (7)$$

where we took the limit of large interdot separation: for $L \gg \hbar u/E_1, \hbar u/E_2$, the scattering probability still has an oscillatory L dependence, $\sin^2(\Delta EL/\hbar u)$, due to interference between processes with plasmon emission at the source and at the probe dot, respectively. This interference disappears once

the energy loss ΔE is averaged over the widths \hbar/τ_i of the dot levels. For $L/u \gg \tau_i$, this energy average leads to a replacement of the \sin^2 factor by its average of $1/2$, and the result Eq. (7) is obtained. We note that the criterion on L for the disappearance of the oscillatory factor agrees with the criterion for fixing the time ordering on the Keldysh contour used to derive Eq. (3).

Using Fermi's golden rule, the tunneling current is obtained as $I = (-e_0 2\pi/\hbar) \int \frac{dp}{2\pi} |\langle f|i\rangle|^2 u \delta(\Delta E - u|p|)$. It correctly reproduces the inelastic component, $I_{\text{inel}} \propto \gamma/\Delta E$, of Eq. (6) to order $\gamma \approx g_2^2/(4\pi\hbar u)^2$. Finally, we note that the matrix element in Eq. (7) scales as $1/\sqrt{|\Delta E|}$. This can be understood by multiplying the matrix element for plasmon emission, which increases as $\sqrt{|\Delta E|}$, with the time available for plasmon emission, which diminishes as $1/|\Delta E|$ due to the energy-time uncertainty principle.

Next, we consider tunneling into a chiral LL at the edge of a fractional quantum-Hall state from the Laughlin sequence. We focus on the filling fraction $\nu = 1/3$, where the area occupied by one electron is threaded by three quanta of magnetic flux. The current for the chiral LL can be derived in a similar fashion as in the standard case. First, we note that the Hamiltonian is analogous to that in Eq. (1), but with only one boson field, say ϕ_R , and with K replaced by the filling fraction ν . The tunneling Hamiltonian is identical to Eq. (2), and the electron operator is now bosonized as $\psi(x) = e^{i\phi_R(x)/\nu}/\sqrt{2\pi\alpha}$. Using similar steps as above, one finds

$$I = e_0 |\eta_1|^2 |\eta_2|^2 \int_{-\infty}^{\infty} dt_2 dt_3 dt_4 e^{-iE_2 t_2 + iE_1 t_3} [iG_{1/\nu}^<(t_2)] \times [iG_{1/\nu}^>(t_3)] \{\Pi_{1/\nu}^< - \Pi_{1/\nu}^<<\}. \quad (8)$$

The correlation functions and the Π matrices are again given by Eqs. (4) and (5). Performing the time integrals in Eq. (8) exactly, we obtain

$$I = -e_0 \frac{\pi^3 |\eta_1|^2 |\eta_2|^2 \alpha^4 (k_B T)^3}{4u^6 \hbar^7} \left[\frac{X_1^2 e^{X_1/2}}{\cosh(X_1/2)} \left(1 + \frac{X_1^2}{\pi^2} \right) \delta(\Delta X) + \frac{3\Delta X e^{\Delta X/2}}{\sinh(\Delta X/2)} \sum_{i=1}^2 \frac{e^{X_i/2}}{\cosh(X_i/2)} \left(1 + \frac{X_i^2}{\pi^2} \right) \right]. \quad (9)$$

Here, $\Delta X = X_1 - X_2$ and $X_i = E_i/k_B T$. At zero temperature, the expression for the current simplifies to $I \propto E_1^4 \delta(\Delta E) + 6\theta(\Delta E)(E_1^2 + E_2^2)\Delta E$. The current, plotted for both zero and finite temperatures in Fig. 3, has two main contributions: elastic and inelastic. The peak is due to electrons that were elastically transported from the source to the probe. Second, there is a broad inelastic contribution that extends over the range $E_2 < E_1$ and that grows monotonically as E_2 is lowered. For $E_2 \approx E_1$, the current increases linearly with ΔE . We have confirmed that a similar inelastic contribution to the current is also present for the Laughlin filling fraction $\nu = 1/5$. In this case, an exact computation at zero temperature shows again that $I_{\text{inel}} \propto \Delta E$ for $E_2 \lesssim E_1$. This suggests that the linear upturn in the current below E_1 may be a generic feature at all Laughlin filling fractions.

For a noninteracting chiral Fermi liquid, which describes the edge excitations of an integer quantum-Hall state, hot

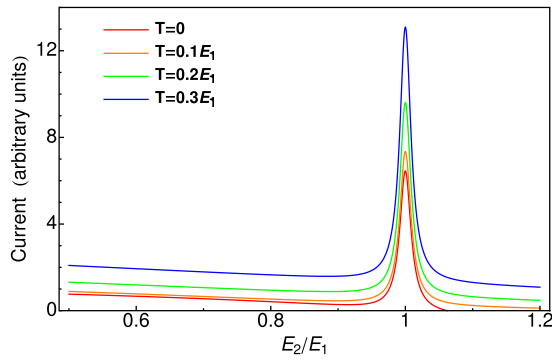


FIG. 3. (Color online) The tunneling current for the chiral LL at various temperatures. It shows an elastic contribution at $E_1 = E_2$ and an inelastic contribution for $E_2 < E_1$. The same level broadening is used for the elastic peak as in the standard case.

electrons do not relax. In addition, the weight of the elastic peak is reduced as the temperature is increased. This reduction is due to Pauli blocking of states by thermally excited edge electrons residing above the chemical potential. When interactions are present, Fig. 3 shows an overall increase in the elastic current with temperature. This reflects the increase in the tunneling density of states with temperature and constitutes a clear signature of LL physics.

The setup of Fig. 1 is ideal for directly extracting the electron energy distribution, $f(E)$, and spectral function, $A(E)$, inside the wire at a spatial point far from the injection site. With the probe occupancy constrained to be empty, the tunneling current is given by $I_{\text{empty}} = ie_0 |\eta_2|^2 G^<(E)$, while a similar evaluation with probe occupation held full gives $I_{\text{full}} = ie_0 |\eta_2|^2 G^>(E)$.²⁴ Once the two currents are obtained, both $f(E)$ and $A(E)$ can be extracted by expressing the lesser and greater Green functions, $G^<(E) = if(E)A(E)$ and $G^>(E) = -i[1 - f(E)]A(E)$, in terms of electron distribution function

and spectral weight. At zero temperature and for $\nu = 1/3$, $f(E_2)$, and $A(E_2)$ valid for $0 < E_2 < E_1$ read

$$A(E_2) = \frac{\alpha^2}{2u^3 \hbar^4} \left[E_2^2 + (E^*)^2 \frac{\Delta E}{E_1} \right], \quad (10)$$

$$f(E_2) = \frac{[1 + (E_2/E_1)^2](\Delta E/E_1)}{(E_2/E^*)^2 + (\Delta E/E_1)}, \quad (11)$$

where $E^* = \sqrt{6\pi |\eta_1|^2 \alpha^2 E_1^3 / u^3 \hbar^3}$ separates two energy regimes. We note that E^* can be parametrically larger than the level widths such that our sequential tunneling approximation stays valid. In the high-energy regime and for small energy transfers ($E^* \ll E_2 \leq E_1$), $f(E_2) \approx 12\pi |\eta_1|^2 \alpha^2 \Delta E / u^3 \hbar^3$, which shows that the linear upturn in the current below E_1 is also reflected in the distribution function. In the same regime, we find that the spectral function does not deviate strongly from its equilibrium expression (with $\eta_1 = 0$). In the low-energy regime ($0 \leq E_2 < E^*$), $f(E_2)$ smoothly approaches one and the spectral function approaches a finite value. The latter is in stark contrast to the equilibrium case.

In conclusion, we have theoretically addressed how locally injected electrons can relax inside a LL. For the standard LL, the locality of the injection and collection processes allows electrons to tunnel into virtual momentum states and then to relax through plasmon emission. In chiral LLs, the tunnel current into the detector quantum dot increases when lowering the detection energy, in contrast to the decreasing tunneling density of states, thus providing evidence that the strength of energy relaxation is determined by many-body dynamics and not just by density-of-states effects.

The authors would like to thank Amir Yacoby for drawing our attention to the problem of local and energy resolved electron injection. B.R. acknowledges support from the Heisenberg program of DFG.

¹D. C. Mattis and E. H. Lieb, *J. Math. Phys.* **6**, 304 (1965).

²T. Giamarchi, *Quantum Physics in One Dimension* (Oxford University Press, Oxford, 2003).

³X.-G. Wen, *Phys. Rev. B* **41**, 12838 (1990).

⁴X.-G. Wen, *Phys. Rev. Lett.* **64**, 2206 (1990).

⁵C. L. Kane and M. P. A. Fisher, *Phys. Rev. B* **46**, 15233 (1992).

⁶T. Lorenz *et al.*, *Nature (London)* **418**, 614 (2002).

⁷O. M. Auslaender *et al.*, *Science* **308**, 88 (2005).

⁸K. Le Hur, B. I. Halperin, and A. Yacoby, *Ann. Phys.* **323**, 3037 (2008).

⁹H. Steinberg *et al.*, *Nat. Phys.* **4**, 116 (2008).

¹⁰M. Bockrath *et al.*, *Nature (London)* **397**, 598 (1999).

¹¹Z. Yao, H. W. Ch. Postma, L. Balents, and C. Dekker, *Nature (London)* **402**, 273 (1999).

¹²F. P. Milliken, C. P. Umbach, and R. A. Webb, *Solid State Commun.* **97**, 309 (1996).

¹³A. M. Chang, L. N. Pfeiffer, and K. W. West, *Phys. Rev. Lett.* **77**, 2538 (1996).

¹⁴M. Grayson, D. C. Tsui, L. N. Pfeiffer, K. W. West, and A. M.

Chang, *Phys. Rev. Lett.* **86**, 2645 (2001).

¹⁵Y.-F. Chen, T. Dirks, G. Al-Zoubi, N. O. Birge, and N. Mason, *Phys. Rev. Lett.* **102**, 036804 (2009).

¹⁶D. B. Gutman, Y. Gefen, and A. D. Mirlin, *Phys. Rev. B* **80**, 045106 (2009).

¹⁷D. A. Bagrets, I. V. Gornyi, and D. G. Polyakov, *Phys. Rev. B* **80**, 113403 (2009).

¹⁸S. Ngo Dinh, D. A. Bagrets, and A. D. Mirlin, *Phys. Rev. B* **81**, 081306(R) (2010).

¹⁹S. Pugnetti, F. Dolcini, D. Bercioux, and H. Grabert, *Phys. Rev. B* **79**, 035121 (2009).

²⁰M. Khodas, M. Pustilnik, A. Kamenev, and L. I. Glazman, *Phys. Rev. B* **76**, 155402 (2007).

²¹C. Altimiras, H. le Sueur, U. Gennser, A. Cavanna, D. Mailly, and F. Pierre, *Nat. Phys.* **6**, 34 (2010).

²²J. Rammer and H. Smith, *Rev. Mod. Phys.* **58**, 323 (1986).

²³C. L. Kane and M. P. A. Fisher, *Phys. Rev. B* **67**, 045307 (2003).

²⁴C. de C. Chamon and X. G. Wen, *Phys. Rev. Lett.* **70**, 2605 (1993).